# Mitigation of Atmospheric Turbulences Using Mode Division Multiplexing based on Decision Feedback Equalizer for Free Space Optics

**Article** *in* Journal of Optical Communications · January 2017

DOI: 10.1515/joc-2017-0169



**3 authors:**

Abdullah Almogahed
Universiti Utara Malaysia


Angela Amphawan
Massachusetts Institute of Technology


Yousef Fazea
Universiti Utara Malaysia

Abdullah Almogahed, Angela Amphawan and Yousef Fazea*

# Mitigation of Atmospheric Turbulences Using Mode Division Multiplexing based on Decision Feedback Equalizer for Free Space Optics

https://doi.org/10.1515/joc-2017-0169
Received September 26, 2017; accepted October 25, 2017

**Abstract**: In mode division multiplexing (MDM) free space optical (FSO) communication system, the atmospheric turbulences such as fog, rain, and haze cause adverse effects on system performance. This paper investigates the mitigation of atmospheric turbulences of FSO using MDM and decision feedback equalizer (DFE) with minimum mean square error (MMSE) algorithm. The implementation of the MMSE algorithm is used to optimize both the feedforward and the feedback filter coefficients of DFE. The proposed system comprises three parallel 2.5Gbit/s channels using Hermite–Gaussian modes. A data rate of 7.5Gbit/s over 40 m, 800 m, 1400 m, and 2km under medium fog, rain, haze, and clear weather, respectively, has been achieved. In addition, it is noticed that the link distance is reduced while increasing the attenuation. The simulation results revealed that a DFE improves the performance MDM FSO system while maintaining high throughput and desired low bit error rate.

**Keywords**: atmospheric turbulence, decision feedback equalization, mode division multiplexing, free space optics

## Introduction

In the last decade, the mobile devices and applications spread widely, as well as a remarkable growth of users who use them around the world are increasing day by day, largely resulting in the increasing demand for the bandwidth of wireless networks in an unprecedented way [1]. According to tenth annual Cisco Visual Networking Index report [2], the expected global mobile data traffic will tremendously increase eightfold from 2015 to 2020. This increase in the mobile data traffic will lead to increasing demand for bandwidth and high-speed data transmission as well [3].

Radio frequency (RF) spectrum is not a longer appropriate solution to meet the growing demand for bandwidth [4–6] because of several limitations in terms of cost, security, noise, and bandwidth. RF is more expensive because it requires a license to operate. In addition, RF is less secure as a result of the exposing for eavesdropping or intercepting [6]. RF suffers from interference issue that causes noise to the signal [2, 7]. In addition, the bandwidth in RF is limited in the range of 10 Mbps to several 100 Mbps [4, 5].

As a result of those RF limitations, switching to an alternate solution, which can provide higher data rate and increased bandwidth–distance product, is imperative [2, 4]. Free space optical (FSO) communication is considered as a promising technology to provide a substantial increase of bandwidth–distance product. FSO uses the optical links such as laser between the transmitter and the receiver to transmit data in unguided propagation using free space as a medium [1, 4]. The FSO offers several advantages over RF in terms of cost, security, interference, and bandwidth. It is cheap because it does not require a license to operate in addition to low installation cost [6, 8]. FSO is more secure as a result of difficulty for eavesdropping or intercepting the optical signal which makes it more beneficial to apply in military, financial, and banking domains [5, 8]. FSO guarantees less or no interference between the optical frequencies [5]. Moreover, FSO provides a huge data bandwidth reach up to 2,000 THz because the frequency of the optical carriers lies between 1,012 Hz and 1,016 Hz, in addition to 10 Gbit/s data rate [5].

Furthermore, the FSO guarantees increasing the capacity by using mode division multiplexing (MDM)

***Corresponding author: Yousef Fazea,** Optical Computing and Technology Laboratory, School of Computing, Universiti Utara Malaysia, Sintok, Kedah, Malaysia; InterNetWorks Research Laboratory, School of Computing, Universiti Utara Malaysia, Sintok, Kedah, Malaysia, E-mail: yosiffz@internetworks.my
**Abdullah Almogahed,** Optical Computing and Technology Laboratory, School of Computing, Universiti Utara Malaysia, Sintok, Kedah, Malaysia; Faculty of Engineering and Information Technology, Software Engineering Dep, Taiz University, Taiz, Yemen
**Angela Amphawan,** Optical Computing and Technology Laboratory, School of Computing, Universiti Utara Malaysia, Sintok, Kedah, Malaysia; Research Laboratory of Electronics, Massachusetts Institute of Technology, Cambridge, MA, USA

technology. MDM is a promising technology [9–11] used to transmit the optical signal or light beams in form of modes such as Laguerre–Gaussian mode [12, 13], Hermite–Gaussian (HG) mode [14, 15], helical–phase mode [16, 1718], spot mode, and donut mode [14, 16, 19] through the transmission channel that leads to expand the capacity . This technology has been used over optical fibre and FSO, where it successfully achieved increasing the data capacity. As a result of those features, FSO considers one of the most important technologies that attracts the attention of the next generation of wireless networks, as well as broadband communicating. However, the primary impairment that faces FSO systems and adversely affects its performance is the atmospheric turbulence that causes signal distortion [20].

Several equalization techniques have been proposed in order to mitigate the signal distortion during transmission through free space. The recursive least square (RLS)-based adaptive equalization was proposed by Wang *et al.*, in [21] to remove the intersymbol interference (ISI) and improve the performance the wavelength division multiplexing (WDM) visible light communication (VLC) system. Using RLS has led to improve the WDM–VLC system performance where data rate reaches to 4.5Gbit/s has been transmitted across distance of 1.5 m indoor FSO with error free of $3.8\times10^{-3}$. Bekkali *et al.* in [22] argued that the performance of maximum likelihood sequence estimation (MLSE) equalizers is not satisfactory in the turbulent environment due to the sensitivity to every parameter in the transversal structure. In addition, orthogonal frequency division modulation (OFDM) technique has been introduced in order to make equalization's task more simple. Therefore, experiments on OFDM over FSO have been conducted to prove that OFDM over FSO can be beneficial to design FSO and evaluate its ability for transmission data over its turbulent links under practical condition. Kai Shi *et al.*, in [23], proposed an analytical model to transmit signal based on OFDM over FSO links by taking into consideration the noise of optical signals and nonlinear distortion for the laser diode. A gamma–gamma distribution was used to model the impact of the atmospheric turbulence, which showed an important performance enhancement that can be helpful to design link based on OFDM for data transmission and to alleviate ISI. Advancing this more, many programmable approaches for channel estimation such as minimum mean square error (MMSE) and RLS [24–26] have been proposed alleviate the effects of signal distortion.

In spite of the fact that MDM over FSO has been used to increase the capacity and distance, equalization has not been used to leverage the performance of MDM in FSO [20]. MDM over FSO achieved a data rate of 80 Gbit/s for distance of 1 m by Milione *et al.* [27]. Then, 280 Gbit/s has been achieved across distance of 5 m using space division multiplexing [28]. To advance this more, this paper investigates the mitigation of the atmospheric turbulences for FSO through using MDM based on DFE.

The remainder of the paper is organized as follows. The system description is discussed followed by mathematical description of the DFE taps using MMSE algorithm. The following section describes the differences between FFF and DFE. This is followed by the description of results and discussions. The final section concludes.

## System description

The proposed MDM FSO with DFE transmission system, modelled in OptSim 5.2, is illustrated in Figure 1. Three independent non-return-to-zeros (NRZ)-encoded channels, each carrying 2.5 Gbit/s, are modulated over an optical spatial carrier by modal multiplexing on three laser modes $HG_{00}$, $HG_{01}$ and $HG_{02}$ that are combined

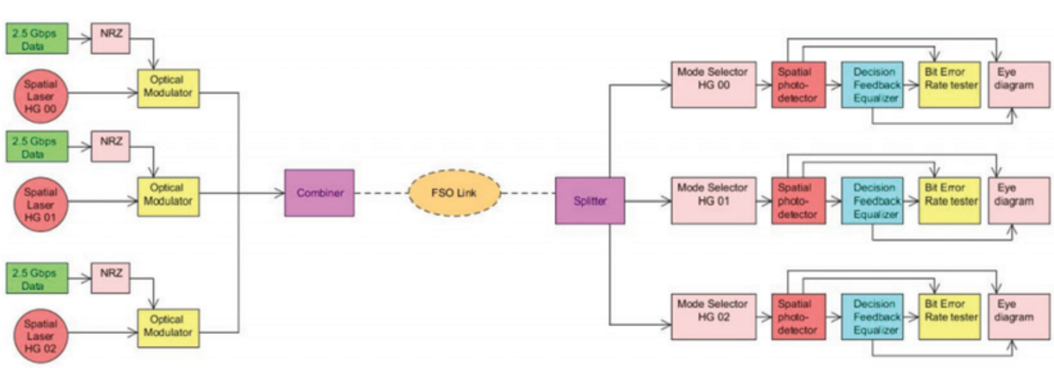


**Figure 1:** Block diagram of DFE in MDM for FSO system.

and transmitted over a FSO link of 40 m, 800 m, 1400 m, and 2 km under medium fog, rain, haze, and clear weather conditions, respectively. The link equation for free space optics [29] is modelled by eq. (1), where $d_R$ defines receiver aperture diameter, $d_T$ is the transmitter aperture diameter, $\theta$ is the beam divergence, and $R$ is the range and $\alpha$ is the atmospheric attenuation.

$$P_{\text{Received}} = P_{Transmitted}\left(\frac{d_R^2 R}{(d_T + \theta R)^2}\right)10^{-\alpha R/2} \tag{1}$$

At the receiver side, the transmitted mode is extracted based on optical splitter. The output mode is then fed to a spatial photo detector followed by DFE to retrieve the original baseband signal. Bit error rate (BER) tester and eye diagram analyser are used to evaluate the performance MDM FSO system before and after DFE scheme. The simulation parameters are listed in Table 1.

**Table 1:** Simulation parameters for DFE in MDM for FSO system.

| Parameters | Values |
|---|---|
| Data rate | 3 × 2.5 Gbps |
| Transmitted wavelength | 850 nm |
| Link range | 40 m –2km |
| Beam divergence | 2 murd |
| Transmitter's and receiver's apertures | 20 cm |
| Data rate | 3 × 2.5 Gbps |

The attenuation is considered one of the main parameters, which are limiting the FSO systems' performance. Typically, the values of attenuation are changing with change in the atmospheric conditions. The attenuation reduces the signal power at the receiver side. Table 2 illustrates the values of attenuation for various weather conditions [2].

**Table 2:** The values of attenuation for various weather conditions.

| Weather conditions | Attenuation in dB/km |
|---|---|
| Clear weather | –0.155 |
| Medium haze | –4.285 |
| Medium rain | –9.64 |
| Medium fog | –33.961 |

## Optimizing DFE taps using MMSE algorithm

The MMSE algorithm jointly optimizes the settings of both the feed-forward filter (FFF) taps and the feedback filter (FBF) taps of DFE to minimize the mean square error (MSE) [30]. The way to calculate the best taps is to approach the problem from a perspective where all that matters is getting the best signal. That will be done by choosing the taps that minimize the difference between the equalized signal and the transmitted (or ideal) signal [31].

The overall channel input/output relationship is given by eq. (2), where $y_k$ is the channel output, $h_i$ is the channel pulse response, $x_i$ is the channel input, $n_k$ is the noise sequence, $k$ is the estimated time, and $v$ is the channel memory.

$$y_k = \sum_{i=0}^{v} h_i x_{k-i} + n_k \tag{2}$$

The DFE filters have finite lengths and can be represented as vectors. The FFF consists of $N_f$ taps vector denoted by $w$, where $w = \left[w_0, w_1, \ldots w_{N_f-1}\right]^T$ and FBF consists of $N_b$ taps vector denoted by $b$, where $b = \left[b_0, b_1, \ldots b_{N_f-1}\right]^T$. Choosing w and b for optimizing performance of the MMSE–DFE according to a chosen performance criterion represents our objective. The MSE will be adopted as our index for the performance, the error sequence, $e_k$, is given by eq. (3), where $Z_k$ is the output of FFF and Δ indicates to the decision delay.

$$\begin{aligned} e_k &\overset{def}{=} x_{k+N_{f-1-\Delta}} - z_k = x_{k+N_{f-1-\Delta}} \\ &- \sum_{i=0}^{N_{f-1}} w^{\star}_{-i} y_{k+i} + \sum_{j=1}^{N_b} b_j^{\star} x_{k+N_{f-1-\Delta-j}} \end{aligned} \tag{3}$$

$$= [0_{1\times\Delta 1} b_1^{\star} \ldots b_{N_b}^{\star} 0_{1\times s}] x_{k+N_{f-1:k-v}} -$$

$$[w^{\star}_{-(N_{f-1})} \ldots w_0^{\star}] y_{k+N_{f-1:k}} \overset{def}{=} \tilde{b}^{\star} x_{k+N_{f-1:k-v}} - w^{\star} y_{k+N_{f-1:k}} \tag{4}$$

Therefore, MSE is given by:

$$MSE \overset{def}{=} E\left[|e_k|^2\right] = E\left[\begin{array}{c}\left(\tilde{b}^{\star} x_{k+N_{f-1:k-v}} - w^{\star} y_{k+N_{f-1:k}}\right)\cdot \\ \left(\tilde{b}^{\star} x_{k+N_{f-1:k-v}} - w^{\star} y_{k+N_{f-1:k}}\right)\end{array}\right] \tag{5}$$

If we make the following definitions, where $R_{xx}$ and $R_{nn}$ represent the autocorrelation matrices of the channel input and noise sequences, and $H$ is the Toeplitz matrix of channel coefficients.

$$R_{xy} \overset{def}{=} E\left[x_{k+N_{f-1:k-v}} y^{\star}_{k+N_{f-1:k}}\right] = R_{xx} H^{\star} \tag{6}$$

$$R_{yy} \overset{def}{=} E\left[y_{k+N_{f-1}} y^{\star}_{k+N_{f-1:k}}\right] = H R_{xx} H^{\star} + R_{nn} \tag{7}$$

Then eq. (5) becomes:

$$MSE = \tilde{b}^{\star} R_{xx} \tilde{b} - \tilde{b}^{\star} R_{xy} w - w^{\star} R_{yx} \tilde{b} + w^{\star} R_{yy} w \tag{8}$$

In minimizing the MSE, we will make use

$$E\left[e_k y^{\star}_{k+N_{f-1:k}}\right] = 0 \Rightarrow \tilde{b}^{\star} R_{xy} = w^{\star} R_{yy} \tag{9}$$

Combining eqs. (8) and (9)

$$MSE = \tilde{b}^{\star} R^{\perp}_{x/y} \tilde{b} \tag{10}$$

where

$$R_{x/y^{\perp}} \stackrel{def}{=} R_{xx} - R_{xy} R_{yy}^{-1} R_{yx} = R_{xx} - R_{xx} H^{\star} (H R_{xx} H^{\star} + R_{nn})^{-1} H R_{xx} = [R_{xx}^{-1} + H^{\star} R_{nn}^{-1} H]^{-1} \tag{11}$$

The last line follows from the matrix inversion lemma' (assuming that $R_{xx}$ and $R_{nn}$ are invertible). By defining:

$$R_{\Delta} \stackrel{def}{=} [0_{(N_b+1)\times\Delta} I_{N_b+1} 0_{(N_b+1)\times s}] R^{\perp}_{x/y} \begin{pmatrix} 0_{\Delta\times(N_b+1)} \\ I_{N_b+1} \\ 0_{s\times(N_b+1)} \end{pmatrix}$$

$$MSE = [1 b_1^{\star} \ldots b_{N_b}^{\star}] R_{\Delta} \begin{pmatrix} 1 \\ b_1 \\ \cdot \\ \cdot \\ \cdot \\ b_{N_b} \end{pmatrix} \tag{12}$$

This is a quadratic form that is minimized by choosing the FBF settings as follows:

$$b \stackrel{def}{=} [1 b_1 \ldots b_{N_b}]^t = \frac{R_{\Delta}^{-1} e_0}{e_0^t R_{\Delta}^{-1} e_0} \tag{13}$$

Resulting in MMSE to

$$MMSE = \frac{1}{e_0^t R_{\Delta}^{-1} e_0} \tag{14}$$

The optimum FFF $w^{\star}_{opt}$ is calculated using eq. (9) as follows: $w^{\star}_{opt} = \tilde{b}^{\star}_{opt} R_{xy} R_{yy}^{-1}$ getting the best performance for DFE depends on the number of FFF and FBF taps that use to recover the original signal. In OptSim 5.2, the possible number of FFF taps ranges between 1 and 100, whereas the possible number of FBF taps ranges between 0 and 100.

# Results and discussion

The performance of DFE in MDM for FSO system has been evaluated using the quantitative BER and qualitative eye diagram metrics with respect to the distance under the four weather conditions.

## Clear weather condition

The attenuation value for clear weather is −0.155 dB/km. Transmission 7.5 Gbit/s of data can be successfully achieved for distance 2 km through FSO link under clear weather condition. A number of FFF and FBF taps for DFE was changed three times to investigate and obtain the best performance. Table 3 shows the BER for each channel before DFE and after different schemes for DFE.

It is noticed that, as shown in Figure 2 and Table 3, the DEFs with two FFF and two FBF taps have shown a significant improvement. However, the FFE two taps are not sufficient to correct all distortion due to the fact that one tap corrects only one bit. Therefore, the output of two FFF taps is added to the logic decision and feedback loop for achieving an additional correction. By applying this process to the three different DFE schemes, the system can cancel more distortion.

Figure 2 shows the eye diagram for each channel before and after DFE at the receiver side once the number of FFF taps is two and FBF taps is two as well. Clear and wide eye diagrams after DFE show successful transmission of 7.5 Gbit/s data with an acceptable signal to noise ratio (SNR) for a distance of 2 km under clear weather.

## Medium haze weather condition

The attenuation value for medium haze is −4.285 dB/km. At medium haze, transmission 7.5Gbit/s of data can be successfully achieved for distance 1400 m through FSO link. Table 4 demonstrates the BER for each channel before DFE and after different schemes for DFE.

**Table 3:** The BER before the DFE and after different scheme of the DFE in clear weather.

| Channels | BER before DEF | BER after Different Schemes of the DFE | | |
|---|---|---|---|---|
| | | DFE Scheme 1 (FFF = 2 and FBF = 1) | DFE Scheme 2 (FFF = 2 and FBF = 2) | DFE Scheme 3 (FFF = 2 and FBF = 3) |
| Channel-1 (HG00) | $3.1972\times10^{-3}$ | $2.6112\times10^{-20}$ | $3.4280\times10^{-28}$ | $1.2007\times10^{-18}$ |
| Channel-2 (HG01) | $3.8090\times10^{-3}$ | $6.5022\times10^{-16}$ | $7.4919\times10^{-18}$ | $6.8280\times10^{-13}$ |
| Channel-3 (HG02) | $2.7905\times10^{-3}$ | $6.8386\times10^{-16}$ | $2.9003\times10^{-20}$ | $1.8103\times10^{-13}$ |

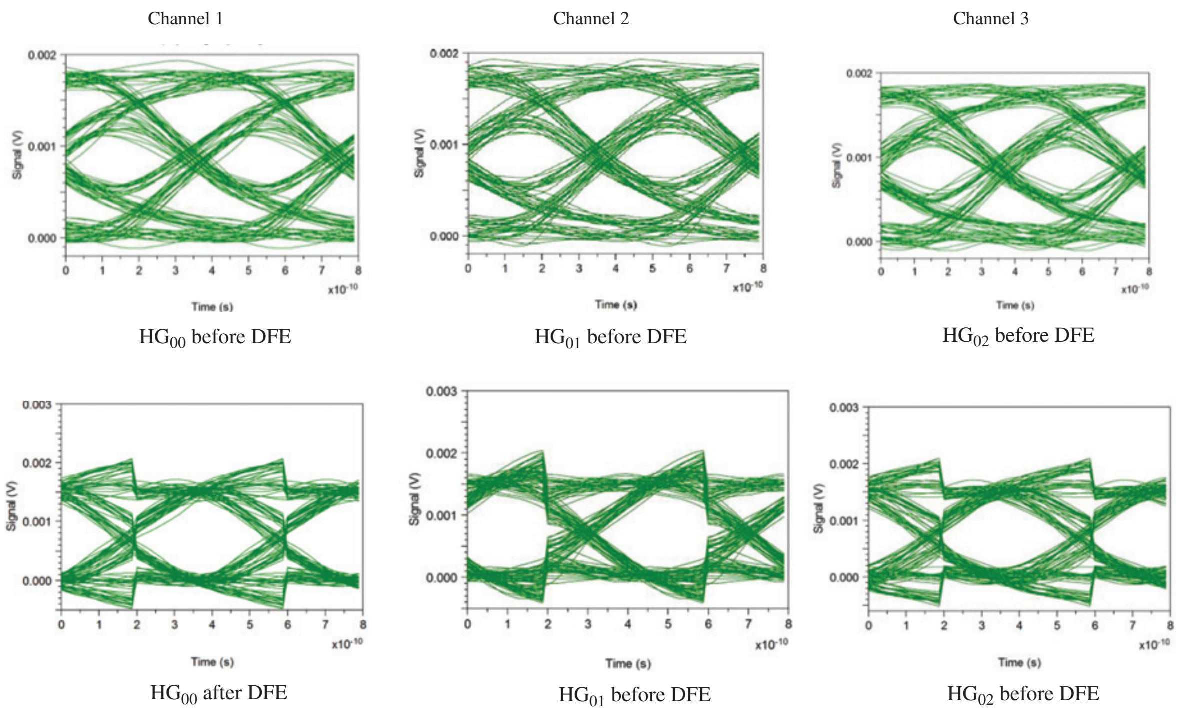


**Figure 2:** Eye diagrams at the receiver side for each channel before and after DFE in case of number of FFF taps is 2 and FBF taps is 2 in a clear weather condition successfully transmitting 7.5 Gbit/s over a distance of 2 km.

**Table 4:** The BER before DFE and after different schemes of the DFE in medium haze weather.

| Channels | BER before DEF | BER after Different Schemes of the DFE | | |
|---|---|---|---|---|
| | | DFE Scheme 1 (FFF = 3 and FBF = 3) | DFE Scheme 2 (FFF = 4 and FBF = 3) | DFE Scheme 3 (FFF = 5 and FBF = 4) |
| Channel 1 ($HG_{00}$) | $3.6109 \times 10^{-3}$ | $4.7305 \times 10^{-19}$ | $3.6296 \times 10^{-19}$ | $6.9784 \times 10^{-29}$ |
| Channel 2 ($HG_{01}$) | $4.5824 \times 10^{-3}$ | $2.5104 \times 10^{-23}$ | $2.3114 \times 10^{-21}$ | $1.7125 \times 10^{-21}$ |
| Channel 3 ($HG_{02}$) | $3.2919 \times 10^{-3}$ | $9.6590 \times 10^{-19}$ | $1.0556 \times 10^{-17}$ | $2.1817 \times 10^{-20}$ |

As shown in Figure 3 and Table 4, once the number DFE taps increased, less BER is experienced. The DEFs with five FFF and four FBF taps have shown a significant improvement. Figure 3 shows the eye diagram for each channel before and after DFE at the receiver side once the number of FFF taps is five and FBF is four. Clear and wide eye diagrams after DFE show successful transmission of 7.5 Gbit/s data with acceptable SNR at a distance of 1,400 m under medium haze weather.

## Medium rain weather condition

The attenuation value for medium rain is −9.64 dB/km. At medium rain, transmission 7.5 Gbit/s of data can be successfully achieved for distance 800 m through FSO link. A number of FFF and FBF taps for DFE was changed three times to investigate and obtain the best performance. Table 7 demonstrates the BER for each channel before DFE and after different schemes for DFE.

As shown in Figure 4 and Table 5, increasing number DFE taps leads to minimize the BER. The DEFs with six FFF and seven FBF taps have shown significant improvement. Figure 4 shows the eye diagram at the receiver for each channel before and after DFE at the receiver side once the number of FFF taps is six and FBF is seven. Wide eye diagrams after DFE show successful transmission of 7.5 Gbit/s data with acceptable SNR for a distance of 800 m under medium rain weather.

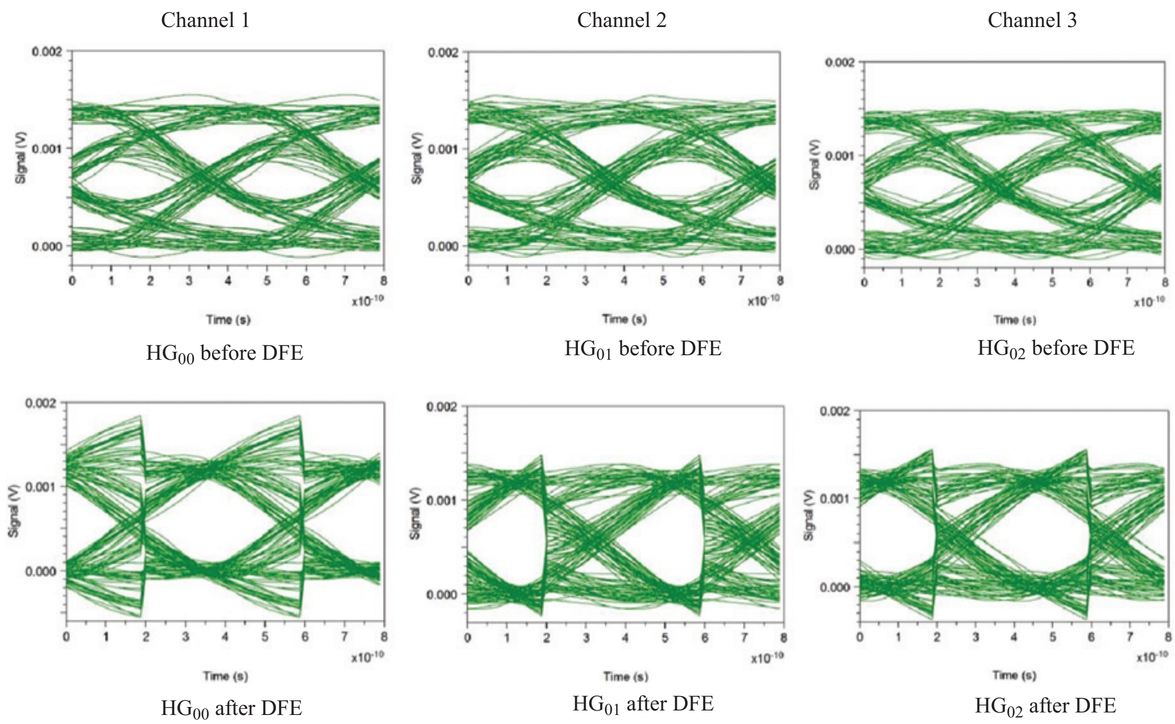


**Figure 3:** Eye diagrams at the receiver side for each channel before and after DFE in case of number of FFF taps is 5 and FBF taps is 4 in a haze weather condition successfully transmitting 7.5 Gbit/s over a distance of 1,400 m.

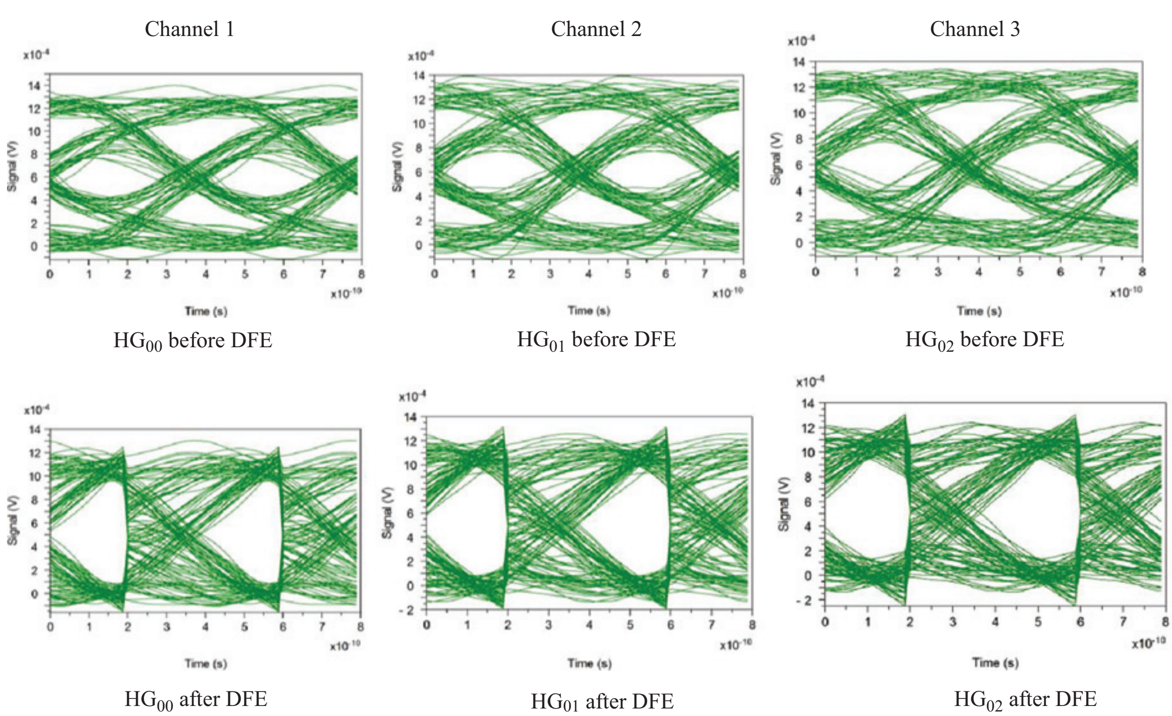


**Figure 4:** Eye diagrams at the receiver side for each channel before and after DFE in case of number of FFF taps is 6 and FBF taps is 7 in a rain weather condition successfully transmitting 7.5 Gbit/s over a distance of 800 m.

**Table 5:** The BER before DFE and after different schemes of the DFE in medium rain weather.

| Channels | BER before DEF | BER after different schemes of the DFE | | |
|---|---|---|---|---|
| | | DFE Scheme 1 (FFF = 5 and FBF = 5) | DFE Scheme 2 (FFF = 5 and FBF = 6) | DFE Scheme 3 (FFF = 6 and FBF = 7) |
| Channel 1 ($HG_{00}$) | $3.9002 \times 10^{-3}$ | $1.6803 \times 10^{-17}$ | $1.6846 \times 10^{-17}$ | $3.0265 \times 10^{-17}$ |
| Channel 2 ($HG_{01}$) | $5.1335 \times 10^{-3}$ | $1.3392 \times 10^{-18}$ | $1.3253 \times 10^{-18}$ | $2.6616 \times 10^{-19}$ |
| Channel 3 ($HG_{02}$) | $3.6583 \times 10^{-3}$ | $6.2747 \times 10^{-16}$ | $3.4754 \times 10^{-16}$ | $2.6890 \times 10^{-17}$ |

### Medium fog weather condition

The attenuation value for medium fog is −33.961 dB/km. The medium fog condition has the highest attenuation factor in atmosphere for laser beam compared to other weather conditions. Generally, it reduces the visibility as well as affects the performance of FSO.

At medium fog, transmission 7.5 Gbit/s of data can be successfully achieved for distance 40 m through FSO link. A number of FFF and FBF taps for DFE are changed three times to investigate and obtain the best performance. Table 6 demonstrates the BER for each channel before DFE and after different schemes for DFE.

It is noticed that, as shown in Figure 5 and Table 6, the DEFs with eight FFF and nine FBF taps have shown significant improvement but less distance has achieved due to the high distortion of the signal. Figure 5 shows the eye diagram at the receiver for each channel before and after DFE at the receiver side once the number of FFF eight is nice and FBF is nine. Wide eye diagrams approximately after DFE show less noise and successful transmission of 7.5 Gbit/s data with acceptable SNR for a distance of 40m under medium fog weather.

## Conclusion

This paper investigates the mitigation of atmospheric turbulences of FSO using MDM and decision feedback equalizer (DFE) with MMSE algorithm under various atmospheric conditions such as clear, medium haze, medium rain, and medium fog. The changes in BER for different atmospheric condition while varying the transmission distance are investigated. It is observed that the link distance is decreased while increasing the attenuation. It is noticed that the medium fog has the highest attenuation, where it significantly reduces the distance to 40 m with 7.5Gbit/s data rate. However, communication link of 800 m, 1400 m, and 2km with 7.5Gbit/s data rate has been successfully achieved under medium rain, medium haze, and clear weather, respectively. The simulation results revealed that MDM–DFE can effectively reduce the effect of atmospheric turbulences and therefore improve BER performance.

## Declaration

*The authors declare that no conflict of interest.*

## Compliance with Ethics Requirements

*This article does not contain any studies with human or animal subjects*

**Table 6:** The BER before DFE and after different schemes of the DFE in medium fog weather.

| Channels | BER before DEF | BER after Different Schemes of the DFE | | |
|---|---|---|---|---|
| | | DFE Scheme 1 (FFF = 6 and FBF = 6) | DFE Scheme 2 (FFF = 8 and FBF = 9) | DFE Scheme 3 (FFF = 12 and FBF = 10) |
| Channel 1 ($HG_{00}$) | $3.1461 \times 10^{-3}$ | $2.4686 \times 10^{-24}$ | $3.9129 \times 10^{-18}$ | $1.2049 \times 10^{-44}$ |
| Channel 2 ($HG_{01}$) | $3.7148 \times 10^{-3}$ | $2.0978 \times 10^{-31}$ | $4.7820 \times 10^{-35}$ | $7.1251 \times 10^{-33}$ |
| Channel 3 ($HG_{02}$) | $2.7309 \times 10^{-3}$ | $2.8162 \times 10^{-28}$ | $1.2354 \times 10^{-30}$ | $1.9199 \times 10^{-22}$ |

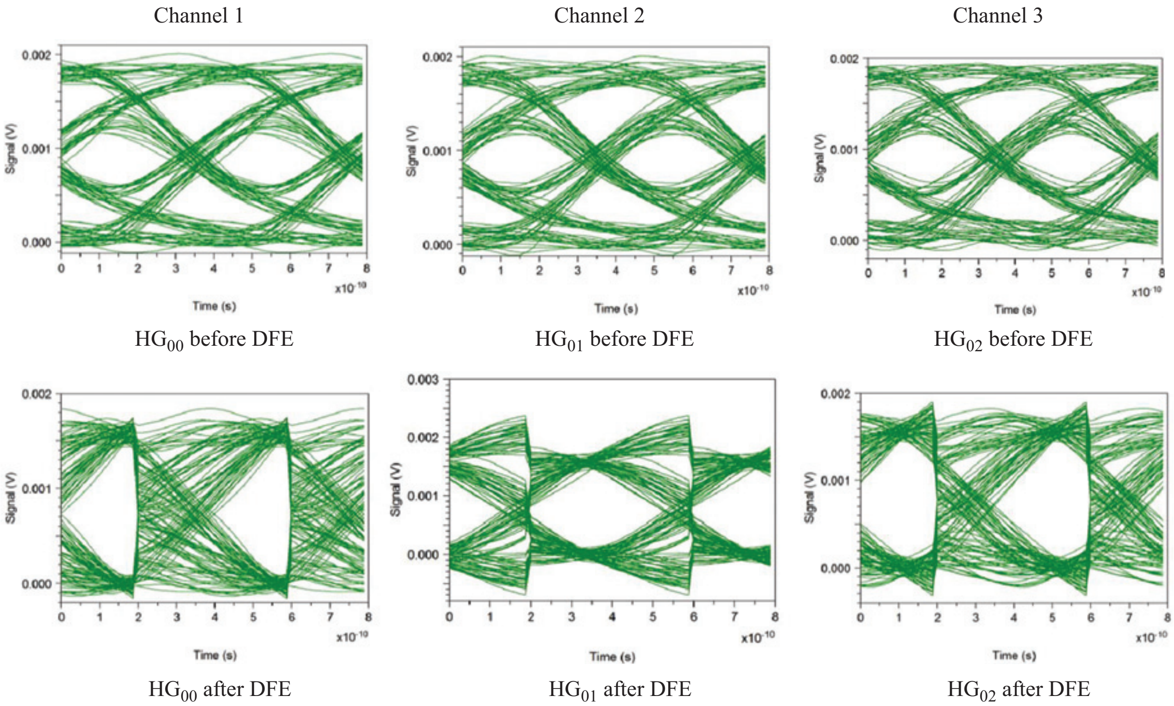


**Figure 5:** Eye diagrams at the receiver side for each channel before and after DFE in case of number of FFF taps is 8 and FBF taps is 9 in a fog weather condition successfully transmitting 7.5 Gbit/s over a distance of 80 m.

## References


1. ISO/IEC, "ISO 27005 information technology security techniques information security risk management.," 2008.
2. Cisco. (FEBRUARY 03, 2016). *10th Annual Cisco Visual Networking Index (VNI) Mobile Forecast Projects 70 Percent of Global Population Will Be Mobile Users*. Available: https://newsroom.cisco.com/press-release-content?articleId = 1741352. Accessed 10 Sep 2017.
3. Kaddoum HK, "Free Space Optical Communication : challenges and Mitigation Techniques," *arXiv preprint arXiv*, pp. 1–28, 2015.
4. Nistazakis HE, Tsiftsis TA, Tombras GS. Performance analysis of free-space optical communication systems over atmospheric turbulence channels. IET Commun. 2009;3:1402–09.
5. Bhatia S, Singh M, Kaushal H, "Performance Analysis in Free Space Optical Communication System Using Aperture Averaging," in *Proceedings of the Second International Conference on Computer and Communication Technologies*, 2016, pp. 319–27.
6. Shah D, Kothari D, "Mitigation of Fog and Rain Effects in Free-Space Optical Transmission Using Combined Diversity," in *Proceedings of the Second International Conference on Computer and Communication Technologies*, 2016, pp. 725–33.
7. AlQuwaiee H, Ansari IS, Alouini M-S. On the maximum and minimum of double generalized Gamma variates with applications to the performance of free-space optical communication systems. IEEE Trans Vehicular Technol. 2016;65:8822–31.
8. Nor NA, Bohata J, Ghassemlooy Z, Zvanovec S, Pesek P, Komanec M, *et al*., "10 Gbps all-optical relay-assisted FSO system over a turbulence channel," in *2015 4th International Workshop on Optical Wireless Communications (IWOW)*, 2015, pp. 69–72.
9. Amphawan A, Fazea Y, Elshaikh M. Space division multiplexing in multimode fiber for channel diversity in data communications. In: Sulaiman HA, et al., editors. Advanced Computer and Communication Engineering Technology. Cham: Springer, 2016:355–63.
10. Amphawan A, Fazea Y, Murad R, Alias H, Sajat M, "MDM of hybrid modes in multimode fiber," *Electrical Engineering, Computer Science and Informatics (EECSI)*, 2015.
11. Fazea Y, Amphawan A. 5 × 5 25 Gbit/s WDM-MDM. J Opt Commun. 2015;36:327–33.
12. Amphawan A, Fazea Y. Laguerre-Gaussian mode division multiplexing in multimode fiber using SLMs in VCSEL arrays. J Eur Opt Society-Rapid Publications. 2016;12:12.
13. Fazea Y, Amphawan A. 40Gbit/s MDM-WDM Laguerre-Gaussian Mode with Equalization for Multimode Fiber in Access Networks. J Opt Commun. 2016. DOI: 10.1515/joc-2016-0138.
14. Amphawan A, Fazea Y. Multidiameter optical ring and Hermite–gaussian vortices for wavelength division multiplexing–mode division multiplexing. Opt Eng. 2016;55:106109–106109.
15. Amphawan A, Fazea Y, Ibrahim H, "Investigation of channel spacing for Hermite-Gaussian mode division multiplexing in multimode fiber," in *2015 IEEE 11th international colloquium on Signal processing & its applications (CSPA)*, 2015, pp. 34–39.
16. Amphawan A, Fazea Y, Elfouly T, Abualsaud K. Effect of vortex order on helical-phased donut mode launch in multimode fiber. Adv Sci Lett. 2015;21:3042–45.

17. Amphawan A, Fazea Y, Ibrahim H, "Mode division multiplexing of spiral-phased donut modes in multimode fiber," in *International Conference on Optical and Photonic Engineering (icOPEN2015)*, 2015, pp. 95240S-95240S.
18. Fazea Y, Amphawan A. Mode division multiplexing of helical-phased LG modes in MMF with electronic dispersion compensation. Adv Sci Lett. 2017;23:29–34.
19. Fazea Y, Amphawan A, Ahmad A, "Spot mode excitation for multimode fiber," in *4th International Conference on Internet Applications, Protocols and Services (NETAPPS2015)*, 2015.
20. Goyal P, Kumar A, Nath V, "Mitigation of atmospheric turbulence in free space optics: a review," in *2015 Fifth International Conference on Advanced Computing & Communication Technologies (ACCT)*, 2015, pp. 634–40.
21. Wang Y, Huang X, Tao L, Shi J, Chi N. 4.5-Gb/s RGB-LED based WDM visible light communication system employing CAP modulation and RLS based adaptive equalization. Opt Express. 2015;23:13626–33.
22. Bekkali A, Ben Naila C, Kazaura K, Wakamori K, Matsumoto M. Transmission analysis of OFDM-based wireless services over turbulent radio-on-FSO links modeled by gamma–gamma distribution. IEEE Photonics J. 2010;2:510–20.
23. Kai Shi FF, Gordon GS, Wilkinson TD, Thomsen BC, " Hybrid Optical/RF Channel Performance Analysis for Turbo Codes," presented at the 2015 IEEE Photonics Conference, 2011.
24. Miller DA. All linear optical devices are mode converters. Opt Express. 2012;20:23985–93.
25. Miller DA. Establishing optimal wave communication channels automatically. J Lightwave Technol. 2013;31:3987–94.
26. Arik SO, Kahn JM, Ho K-P, "MIMO signal processing for mode-division multiplexing: an overview of channel models and signal processing architectures," *IEEE Signal Processing Magazine*, vol. 31, pp. 25–34, 2014.
27. Milione G, Lavery MP, Huang H, Ren Y, Xie G, Nguyen TA, *et al*. $4 \times 20$ Gbit/s mode division multiplexing over free space using vector modes and a q-plate mode (de) multiplexer. Opt Lett. 2015;40:1980–83.
28. Lavery MP, Huang H, Ren Y, Xie G, Willner AE. Demonstration of a 280 Gbit/s free-space space-division-multiplexing communications link utilizing plane-wave spatial multiplexing. Opt Lett. 2016;41:851–54.
29. Refai HH, Sluss JJ, Jr, Refai HH, "The transmission of multiple RF signals in free-space optics using wavelength division multiplexing," in *Defense and Security*, 2005, pp. 136–43.
30. Sur SN, Bera R, Maji B. Decision Feedback Equalization for MIMO Systems. In: Mandal D, Kar R, Das S and Panigrahi BK, editors. Intelligent Computing and Applications. Springer, 2015:205–12, DOI: 10.1007/978-81-322-2268-2_22.
31. Stephens R. Equalization: The Correction and Analysis of Degraded Signal. Santa Clara. Santa Clara, CA: Agilent Technologies. 2005, 12 pages.